water

MDPI

Article

Analyzing Temporal Patterns of Temperature, Precipitation, and Drought Incidents: A Comprehensive Study of Environmental Trends in the Upper Draa Basin, Morocco

Fadoua El Qorchi [1,*], Mohammed Yacoubi Khebiza [1], Onyango Augustine Omondi [2], Ahmed Karmaoui [3], Quoc Bao Pham [4] and Siham Acharki [5]

[1] Laboratory of Water, Biodiversity and Climate Change (WBCC), Department of Biology, Faculty of Sciences Semlalia, Cadi Ayyad University, Marrakech 40000, Morocco; yacoubi@uca.ac.ma
[2] International Center for Climate and Environment Sciences, Institute of Atmospheric Physics, Chinese Academy of Sciences, P.O. Box 9804, Beijing 100029, China; omondagus@gmail.com
[3] Bioactives (Health and Environmental, Epigenetics Team), Faculty of Sciences and Techniques (Errachidia, UMI), Moroccan Center for Culture and Sciences, University Moulay Ismail, Meknes 50050, Morocco; ah.karmaoui@gmail.com
[4] Faculty of Natural Sciences, Institute of Earth Sciences, University of Silesia in Katowice, Będzińska Street 60, 41-200 Sosnowiec, Poland; quoc_bao.pham@us.edu.pl
[5] Department of Earth Sciences, Faculty of Sciences and Technologies of Tangier, University Abdelmalek Essaadi, Tetouan 93000, Morocco; sacharkis@gmail.com or sacharki@uae.ac.ma
* Correspondence: fadoua.elqorchi@ced.uca.ma

Abstract: Quantifying variation in precipitation and drought in the context of a changing climate is important to assess climate-induced changes and propose feasible mitigation strategies, particularly in agrarian economies. This study investigates the main characteristics and historical drought trend for the period 1980–2016 using the Standard Precipitation Index (SPI), Standard Precipitation Evaporation Index (SPEI), Run Theory and Mann–Kendall Trend Test at seven stations across the Upper Draa Basin. The results indicate that rainfall has the largest magnitude over the M'semrir and Agouim (>218 mm/pa) and the lowest in the Agouilal, Mansour Eddahbi Dam, and Assaka subregions (104 mm–134 mm/pa). The annual rainfall exhibited high variability with a coefficient of variation between 35−57% and was positively related to altitude with a correlation coefficient of 0.86. However, no significant annual rainfall trend was detected for all stations. The drought analysis results showed severe drought in 1981–1984, 2000–2001, and 2013–2014, with 2001 being the driest year during the study period and over 75% of both SPEI and SPI values returned drought. Conversely, wet years were experienced in 1988–1990 and 2007–2010, with 1989 being the wettest year. The drought frequency was low (<19%) across all the timescales considered for both SPI and SPEI, with Mansour Eddahbi Dam and Assaka recording the highest frequencies for SPI-3 and SPEI-3, respectively.

Keywords: drought; standardized precipitation index; standardized precipitation evapotranspiration index; precipitation trend; Upper Draa Basin

check for updates

Citation: El Qorchi, F.; Yacoubi Khebiza, M.; Omondi, O.A.; Karmaoui, A.; Pham, Q.B.; Acharki, S. Analyzing Temporal Patterns of Temperature, Precipitation, and Drought Incidents: A Comprehensive Study of Environmental Trends in the Upper Draa Basin, Morocco. *Water* **2023**, *15*, 3906. https://doi.org/10.3390/w15223906

Academic Editor: Paul Kucera

Received: 24 September 2023
Revised: 27 October 2023
Accepted: 28 October 2023
Published: 8 November 2023

1. Introduction

Climate change (CC) is anticipated to alter processes within the water cycle, thereby leading to changes in precipitation patterns that will give rise to weather-related hazards at a local and regional scale [1,2]. For instance, studies show that CC has altered precipitation and temperature over different regions [3–6] and affected hydrological systems [7], leading to an increase in the intensity and frequency of drought and flooding events [8–10]. Drought is a recurring extreme climate event that significantly affects agricultural production, livelihood, and ecological systems, leading to widespread adverse impacts and related losses and damages to nature and people [11]. For example, the global losses from drought increased by $6–8b a year, far more than any other natural disaster [12]. Drought mainly results from water scarcity and can be attributed to various factors, including low precipitation averages, high evapotranspiration rates, the absence of natural water resources, overexploitation of available water resources, or a combination of these factors [13–15]. While drought emanates mainly from a prolonged reduction in precipitation, other climatic variables such as temperature, humidity, and wind speed also play an important role in exacerbating drought conditions by increasing the evapotranspiration rate.

Several studies have revealed significant patterns of temperature increase [16–28], changed rainfall patterns [18,19,23,27,29,30], and alterations in potential evapotranspiration [23,31]. Since 1970, Morocco has experienced a 0.5 °C warming trend per decade, which surpasses the global average of 0.15 °C per decade for the same period [32]. Hartmann et al. [32] argued that despite temperature trends showing an increase of 0.5 °C, regional trends may differ substantially from one region to another. Recent studies have demonstrated that drought has increased in frequency and intensity over Morocco [33–35]. Severe droughts were reported in 1984–1987, 1992–1995, 1998–2003, 2005, 2007–2011, and 2016–2017, with 2008–2011 showing the largest magnitude [36]. Verner et al. [34] estimated that drought-related losses reached $900 million by 1999 and affected over 1 M hectares of arable land, with the 1994–1995 drought alone leading to a loss of 7.9% of the GDP. Likewise, Hartmann et al. [32] reported increased aridity over Morocco and projected a rise in summer drought, particularly in arid and semi-arid regions. Semi-arid areas such as the Upper Draa Basin (UDB) characterized by high precipitation variability are particularly susceptible to drought as their precipitation depends on a few events, and water storage is insufficient to offset the deficits [37]. The UDB has experienced various forms of drought over the past years, leading to water resource shortages [38]. Moreover, the condition is exacerbated by growing population, poor water management, and lack of agreement over shared water resources [34].

Despite lacking a precise definition, drought is generally categorized into four classes, namely, meteorological, agricultural, hydrological, and socioeconomic droughts [38]. Among these classes, meteorological drought is the most common and is considered the initial stage of other drought classes. For this reason, we consider meteorological drought identified by precipitation deficit and possibly made worse by temperatures that favor high evaporation in a region over time. Drought is represented by indices that help determine its multiple characteristics, such as spatial extent, peak intensity, frequency, severity, and duration [39]. Each of these characteristics may have a distinct effect on society and environment. For example, a severe drought with a short duration will have devastating impacts on agricultural activities. In contrast, a prolonged mild drought would have catastrophic consequences on the water supply and ecosystem [40]. Several indices have been developed to quantify drought using different climate parameters [41]. The most commonly used meteorological drought indices are the Standardized Precipitation Index (SPI) [42] and the Standardized Precipitation-Evapotranspiration Index (SPEI) [43]. The SPI index is based on cumulative rainfall probabilities, while SPEI combines potential evapotranspiration (PET) and precipitation to characterize drought. SPEI is one of Europe's most widely used drought indicators [44,45] owing to its ability to incorporate PET, thereby characterizing drought more elaborately. PET is higher than annual precipitation in most arid and semi-arid regions worldwide; therefore, a precipitation-based drought index may not be sufficient to monitor droughts [46]. In regions characterized by minimal temperature fluctuations, the effectiveness of SPI is comparable to that of SPEI [47].

Given the impact of drought on water resource management and sustainable agriculture, several studies have investigated the spatiotemporal variation of rainfall and drought over Morocco. Nevertheless, meteorological drought may vary significantly from one place to another due to high spatial heterogeneity that induces varying responses. Therefore, understanding the variation of rainfall and drought at a regional scale is very important for developing effective countermeasures against the possible consequences of extreme events. Accordingly, the current study investigates rainfall variability, drought characteristics, and their trend over the UDB to understand their dynamics based on SPI and SPEI indices deeply. Specifically, we identify the temporal variation of drought events across the UDB from 1980 to 2016. Such analysis provides a theoretical basis for regional agricultural and ecological management.

2. Materials and Methods

2.1. Study Area

The UDB is located in southeastern Morocco (Figure 1) and covers an approximate area of 15,000 km^2 [48–51]. The main economic activity in the region is agriculture and pastoralism [52]. The altitude of the basin ranges from 4071 m in the high Atlas Mountains to the north, 1100 m–1400 m in the plain of Ouarzazate, and 2500 m in the southern border with Anti-Atlas and Jbel Saghro. The valley is divided into three major basins: the Ouarzazate, Ait Douchen, and Dadès watersheds [50]. Mansour Eddahbi Dam, at the confluence of the Ouarzazate and Dadès Rivers, is the region's primary water supply source. The annual precipitation distribution follows the regions' altitudes and ranges from 104 mm in the plain to 270 mm in the mountains [51]. The temperature distribution also varies with altitude, with an annual maximum temperature as high as 33.8 °C in Mansour Eddahbi Dam and as low as 30 °C in M'semrir. The annual mean of potential evaporation ranges from 4250 m in Assaka to 2570 mm at M'semrir [53].

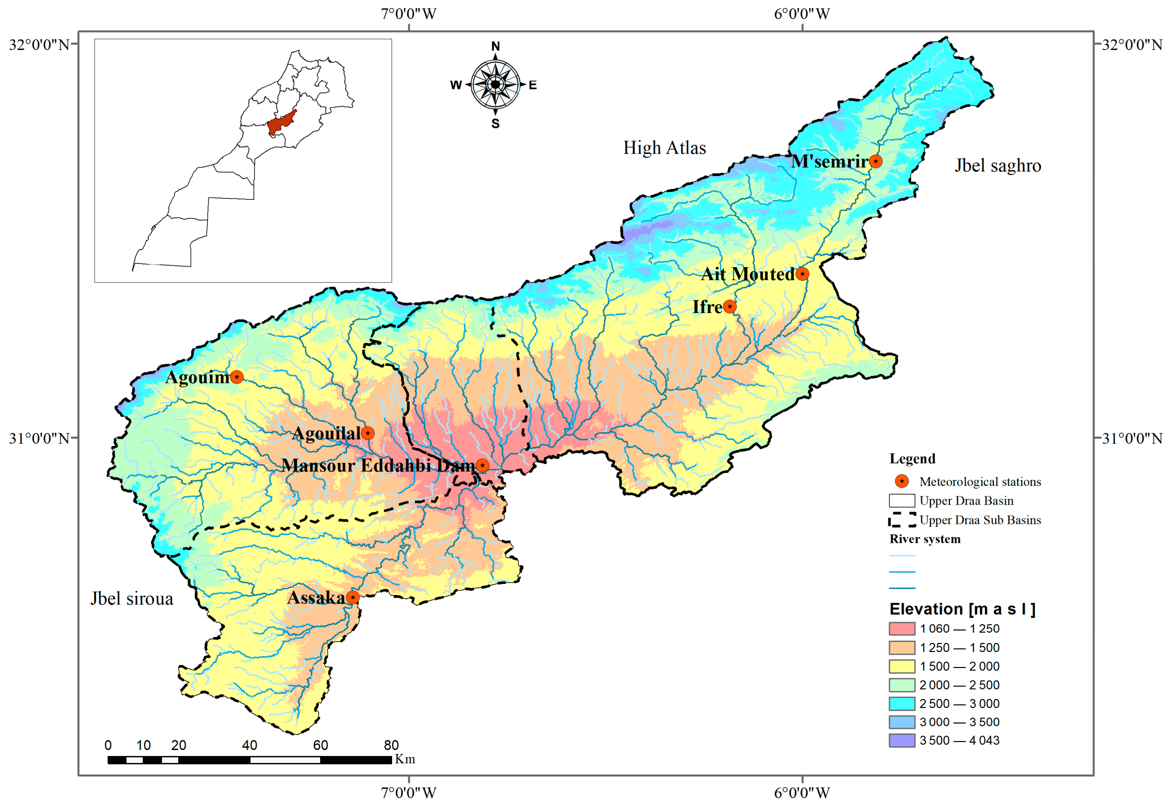

Figure 1. Geographical location, river system, and elevation of the Upper Draa Basin.

2.2. Climate Data

Monthly and annual rainfall and temperature records from 1980 to 2016 for seven synoptic meteorological stations were collected from the Water Basin Agency of Ouarzazate and the Regional Office for Agricultural Development of Ouarzazate. It is worth noting that the 1980–2016 period was chosen due to complete data availability from all seven selected stations, thus enhancing uniformity in our analysis. The seven stations were selected based on their uniform spatial distribution, the availability of maximum data length, and data accuracy (Figure 1).

2.3. Methodology

2.3.1. Trend Analysis

Trend analysis in the context of time series data involves examining the patterns and changes in the data over time. The Mann–Kendall Test (MK Test) has been used to determine significant trends in rainfall, maximum temperature, and minimum temperature (Figure 2). The Z statistic is used to assess a trend's statistical significance, with a positive Z value implying an upward trend and a negative Z value indicating a downward trend [23,54]. Kendall's Tau standardizes the trend between −1 and 1 and is interpreted similarly to the normal approximation Z. Moreover, Sen's slope estimator is another helpful indicator for estimating the actual slope of a monotonous pattern in a time series with a linear trend [54,55]. A Sen's positive slope signifies an upward trend in a time series, while a negative value represents a downward trend [23,54].

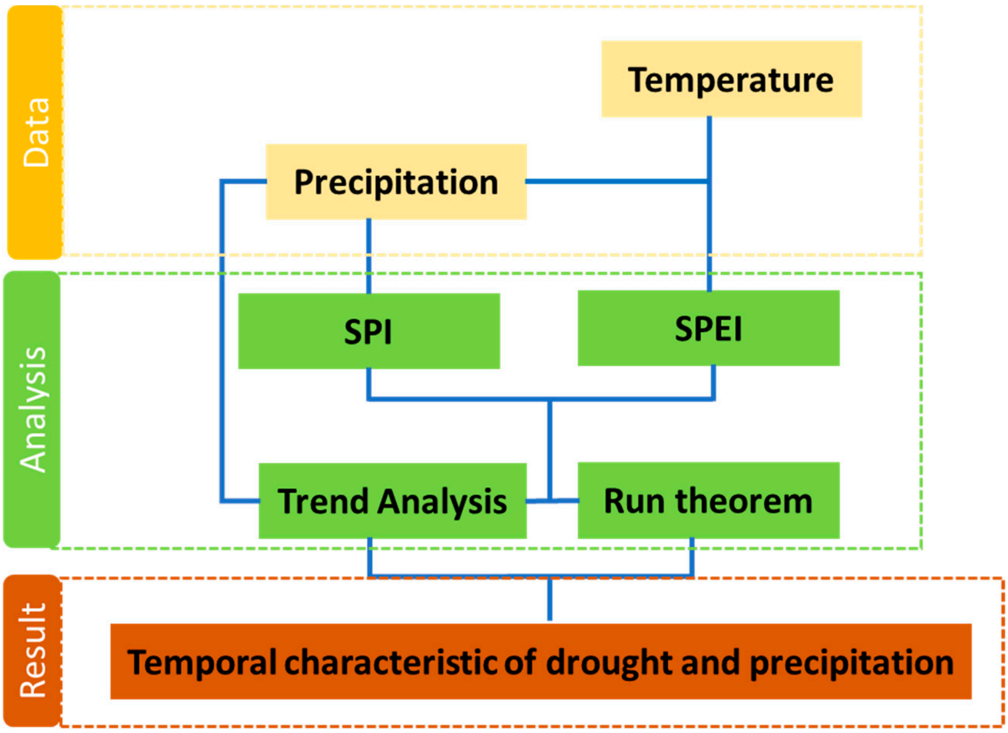

Figure 2. Flowchart methodology.

2.3.2. Drought Indices Analysis

The Standardized Precipitation Index (SPI) as introduced by McKee et al. [42] and the Standardized Precipitation-Evapotranspiration Index (SPEI) developed by Vicente-Serrano et al. [43] have been widely applied for drought analysis [56–59]. SPI assumes that drought emanates from a reduction in rainfall rather than water demand and, therefore, is more closely linked to variability in water cycles. The method for computing SPEI is identical to that of the SPI, with the addition of the evapotranspiration effect through a water balance equation, which may influence drought severity. PET is calculated, subtracted from the monthly rainfall values, and aggregated depending on the chosen timescale. This research used the Hargreaves equation to estimate the PET for SPEI. This method considers both maximum and minimum daily temperature data and the site's latitude. The Hargreave method was chosen due to its simplicity, ease of application, and consistency with methods employed in previous studies [60,61]. The results obtained from the two indices were classified following a predefined threshold proposed by Mckee et al. [42], as shown in Table 1.

Table 1. Classification of drought (or wet) severity events based on SPI/SPEI calculation.

SPI/SPEI Values	Category
2.00 and above	Extremely wet
1.50 to 1.99	Severely wet
1.00 to 1.49	Moderately wet
0.99 to −0.99	Normal
−1.00 to −1.49	Moderate drought
−1.50 to −1.99	Severe drought
−2.0 and less	Extreme drought

2.3.3. Drought Characterization

As presented in Table 1, a drought event is considered any time the SPI or SPEI value is equal to or less than −1 and ends when the index value rises above this threshold [62]. Consequently, the drought basic attributes, i.e., duration, frequency, and severity, were identified using Run Theory (Figure 2). Drought duration was defined as the time when the index value is below the −1 threshold value, and drought severity was defined as a cumulative index value below −1 during the duration of the drought episode, whereas drought intensity was described as a ratio of drought magnitude to its duration.

3. Results and Discussion

3.1. Rainfall and Temperature Variability

The climate of any region is determined by the long-term mean of weather variables, notably temperature and precipitation. Therefore, we describe the climatology of rainfall as well as the maximum and minimum temperatures over the period of study (Figure 3). Figure 3a shows the spatial distribution of rainfall climatology averaged over the study period. The results indicate that rainfall has the largest magnitude over the M'semrir and Agouim (>218 mm/pa) and the lowest in the Agouilal, Mansour Eddahbi Dam, and Assaka subregions (104 mm–134 mm/pa). Ifre and Ait Mouted receive an annual rainfall of 150 mm −190 mm/pa. The difference in annual precipitation may be attributed to local geographical factors, especially the variation in elevation between the High Atlas and Ouarzazate plain, which significantly impacts precipitation.

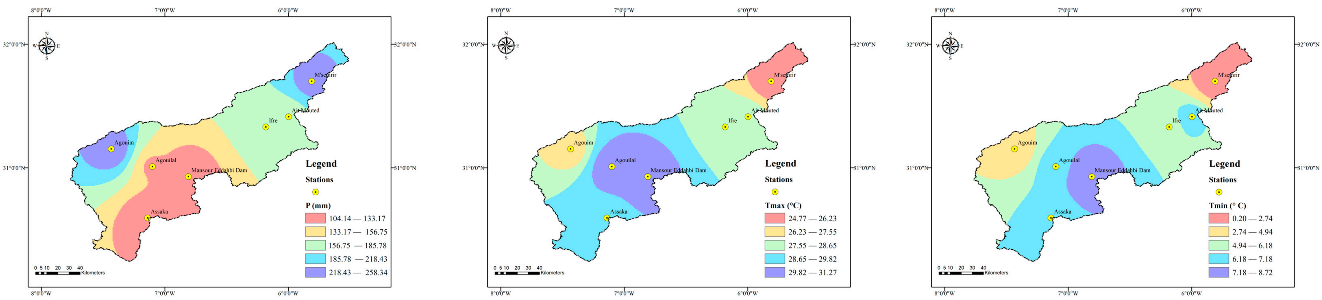

(**a**) (**b**) (**c**)

Figure 3. Descriptive summaries of rainfall (**a**), Tmin (**b**), and Tmax (**c**).

The temperature analysis results reveal that the annual minimum temperature distribution pattern resembles that of the maximum temperature except for the Ait Mouted station, whose minimum temperature tends to be higher than the surrounding stations. The highest annual maximum temperatures (>30 °C) were recorded in Agouilal and Mansour Eddahbi Dam. Conversely, M'semrir recorded the lowest maximum temperature (>25 °C). The results agree with earlier studies by Iqbal et al. [25] and Mishra and Singh [39], which illustrated that the minimum and maximum temperatures decrease as the elevation rises.

Figure 4 shows the relationship between precipitation and altitude. The results indicate that the correlation coefficient between rainfall and altitude is 0.86. The findings are in agreement with earlier studies that showed that precipitation increases with elevation [51,63,64]. Despite this result, it is important to note that large-scale atmospheric patterns significantly influence the rainfall trend observed, alongside the altitude dependence.

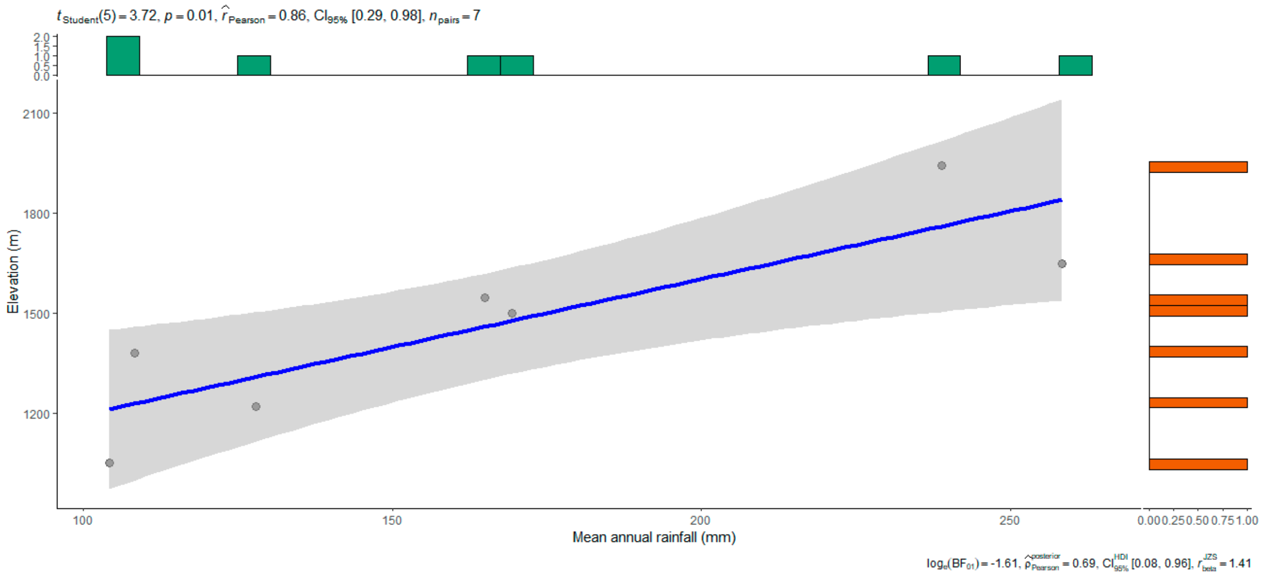

Figure 4. Correlation between mean annual rainfall and elevation. Green and orange represent frequentist analysis and bayesian analysis respectively. Shadow represents the correlation between elevation and mean annual temperature.

The annual variability of rainfall is expressed as the coefficient of variation (CV), calculated as the standard deviation of the annual series divided by the mean and expressed as a percentage. The results indicate that the CV for the annual precipitation ranges from 36.69% to 56.95%. The findings reveal that CV for annual precipitation over the UDB is remarkably high, with CV values surpassing 35%, which agrees with earlier findings by Bouizrou et al. [65]. Indeed, Bouizrou et al. [65] pointed out that the most significant yearly CV values were detected in the semi-arid and desertic climatic zones. Moreover, Alemu and Bawoke [66] and Asfaw et al. [67] indicated that the regions characterized by higher CV in annual precipitation are susceptible to drought.

In contrast, those with elevated CV values are more susceptible to flooding. Moreover, Figure 5 illustrates the monthly average precipitation for the different stations. Results demonstrate that the highest monthly averages were recorded at Agouim (1647 m a.s.l), followed by M'semrir (1942 m a.s.l), then Ifre (1498 m a.s.l), and the lowest monthly average was recorded at Masour Eddahbi Dam (1050 m a.s.l). These monthly averages also exhibit very significant differences throughout the year. Figure 5 shows that July is the least rainy month for all stations. It is noticeable that the average rainfall is less than 10 mm for all stations and reaches its maximum at M'semrir (7.14 mm). The average rainfall during boreal summer is also less than 10 mm for all stations except for M'semrir (21.71 mm) and Agouim (14.79 mm). It is also noticeable that the common characteristic of most stations is a period of dryness in the summer, extending from April to August and sometimes to September (Figure 5).

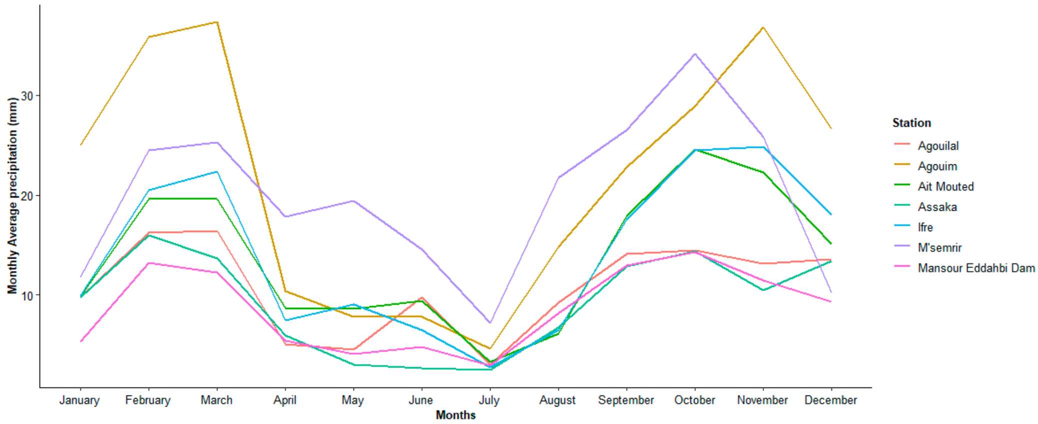

Figure 5. Monthly averages recorded at the UDB.

3.2. Annual and Monthly Trend Analysis

Mann–Kendall Test was performed to determine whether precipitation exhibited a monotonic increasing or decreasing trend over time. Table 2 demonstrates that no significant annual rainfall trend was detected for all stations.

Table 2. Summary of Mann–Kendall Test and Sen's Slope estimator of the annual rainfall.

Rainfall	Mann–Kendall Test				Sen's Slope
	Z	Kendall's Tau	*p*-Value	Trend	
Mansour Eddahbi Dam	0.59	0.07	0.56	No trend	0.63
M'semrir	1.22	0.14	0.22	No trend	1.34
Assaka	−1.22	−0.14	0.22	No trend	−1.35
Ifre	1.02	0.12	0.31	No trend	1.22
Agouim	−0.33	−0.04	0.74	No trend	−0.56
Ait Mouted	1.01	0.12	0.31	No trend	0.92
Agouilal	−0.3	−0.04	0.76	No trend	−0.35

Note: $p < 0.05$ implies a monotonic trend, positive Z signifies an increase, and negative Z indicates a decrease.

The monthly analysis in Table A1 clearly illustrates a decreasing trend for Assaka in January and April. The analysis shows an increase for Ait Mouted and Ifre during September. Nonetheless, no variation has been noticed at Mansour Eddahbi Dam, M'semrir, Agouim, and Agouilal. Table 3 outlines that the minimum temperature for Mansour Eddahbi Dam, Assaka, and Agouilal is increasing annually. The results align with similar studies conducted in other regions of Morocco. For instance, Eddoughri et al. [68] investigated that pattern throughout the agricultural year (1982–2015) and demonstrated significant fluctuations in the Beni Mellal-Khenifra region. The region is also characterized by varying climatic conditions, from humid in the high mountains to semi-arid in the plains, with intensely cold winters and hot summers. Additionally, the average temperature distribution showed fluctuations and a consistent rise in rainfall variability during this period.

Table 3. Summary of Mann–Kendall Test and Sen's Slope estimator for Tmin and Tmax.

Tmin	Mann–Kendall Test				Sen's Slope	Tmax	Mann–Kendall Test				Sen's Slope
	Z	Kendall's Tau	*p*-Value	Trend			Z	Kendall's Tau	*p*-Value	Trend	
Mansour Eddahbi Dam	**4.90**	**0.56**	0.00 *	**Trend detected**	**0.10**	Mansour Eddahbi Dam	0.59	0.07	0.56	No trend	0.01
M'semrir	−1.09	−0.13	0.28	No trend	−0.02	M'semrir	**2.87**	**0.33**	0.00 *	**Trend detected**	**0.04**
Assaka	**3.72**	**0.43**	0.00 *	**Trend detected**	**0.08**	Assaka	**−2.29**	**−0.27**	0.00 *	**Trend detected**	**−0.04**
Ifre	0.98	0.11	0.33	No trend	0.02	Ifre	**3.57**	**0.41**	0.00 *	**Trend detected**	**0.09**
Agouim	0.99	0.13	0.32	No trend	0.03	Agouim	**−2.24**	**−0.29**	0.00 *	**Trend detected**	**−0.07**
Ait Mouted	1.33	0.16	0.18	No trend	0.03	Ait Mouted	**4.80**	**0.56**	0.00 *	**Trend detected**	**0.11**
Agouilal	**4.85**	**0.56**	0.00 *	**Trend detected**	**0.07**	Agouilal	**4.77**	**0.55**	0.00 *	**Trend detected**	**0.08**

Note: * Indicates $p < 0.05$. Bold values are significant at a 95% family-wise confidence level. $p < 0.05$ implies a monotonic trend, positive Z signifies an increase, and negative Z indicates a decrease.

Table A2 in Appendix A reveals that for most months Tmin displays an increase, except for February and November for Mansour Eddahbi Dam. Similarly, Assaka set a rise in the majority of months, except for February, March, September, and October, while the increase was detected only in February and July at Agouim (Table A2) and in April, May, June, August, September, and October for Agouilal. The results were incongruent with the findings of Brahim [69], presenting an upward trend in Tmin. A positive annual trend of Tmax was detected at M'semrir, Ifre, Ait Mouted, and Agouilal (Table 3). Moreover, the monthly increase was detected at M'semrir in April, May, June, July, and August for Ifre in all months except February as well as during all months except in January, February, and December for Ait Mouted, and in January, February, March, and December for Agouilal (Table A3) in Appendix A. However, a negative trend of the Tmax trend was recorded at Agouim and Assaka. The monthly decrease was detected in January and December for Assaka, and in January, March, June, and September for Agouim (Table A3).

The existing temporal patterns and trends within temperature and rainfall time series were evaluated to determine climate variability and change occurrence in the UDB. Overall, the results revealed that temperature variation was more apparent than rainfall.

3.3. Analysis of Drought Characteristics

The SPI and SPEI indices were calculated on 3-, 6-, 9-, and 12-month timescales to evaluate meteorological drought over the UDB (Figure A1) in Appendix A. The temporal changes in the SPEI for the different timescales are presented in Figure A2 in Appendix A. Figure 6 illustrates the contrasting characteristics of the locations of the two stations: Agouim (1647 m a.s.l.), located on the mountains, and Mansour Eddahbi Dam (1050 m a.s.l.), situated on the plain.

Results indicate that Mansour Eddahbi Dam witnessed nine significant dry periods and eleven wet periods, while Agouim encountered eight dry years and fourteen wet periods throughout the study period. The most significant drought period in Agouim corresponds to the peak SPI-12 (−2.82, July 2001), from October 2000 to March 2002, representing 18 months with a severity of 19.87 in Agouim. Conversely, SPI-12 (−3.13, June 2001) from September 2000 to February 2002 represents 17 months with a severity of 29.76 in Mansour Eddahbi Dam. Additionally, Agouim has maximum SPI-3 (2.511), SPI-6 (2.63), SPI-9 (2.55), and Mansour Eddahbi Dam has maximum SPI-3 (2.53), SPI-6 (2.74), SPI-9 (2.42) in November 2014. However, SPI-12 (1.924) was in January 2015 in Agouim, while SPI-12 (2.181) was in December 1989. Confirming these insights, it is noticeable that 2001 was the driest year for most stations, while 2014–2015 had the strongest floods. These findings align with the outcomes of previous studies [51,70,71].

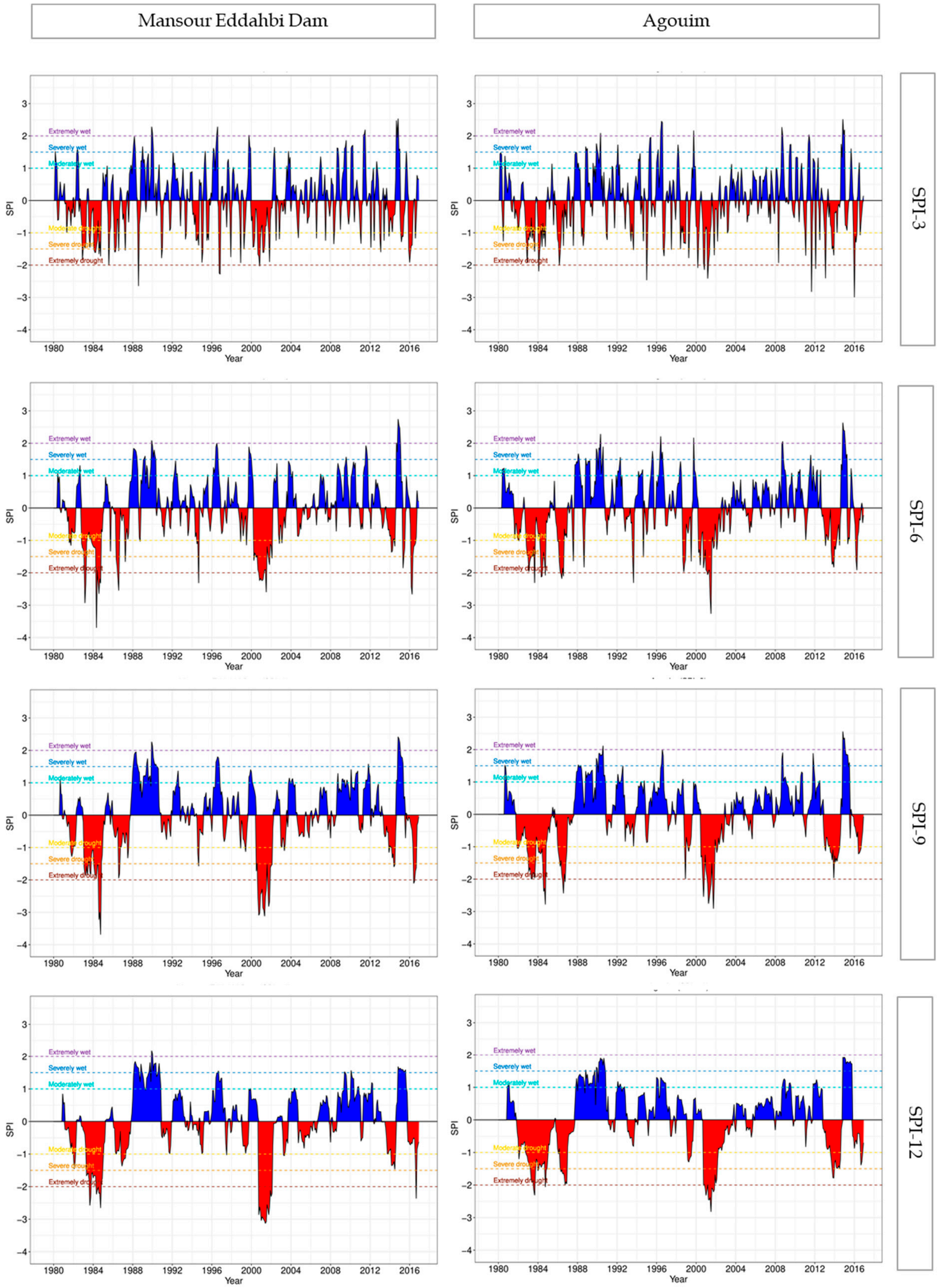

Figure 6. Temporal evolution of SPI values showing wet and dry periods at 3-, 6-, 9-, and 12-month timescales. Red and blue represent dry and wet periods, respectively.

Figure 7 reveals that the temporal evolution of drought calculated using SPEI follows the pattern of SPI. However, compared to SPI, SPEI identified more drought events that were more severe. SPEI identified a multiyear severe drought in 1982–1986 and 2001–2003 in the Mansour Eddahbi Dam and Agouim stations, although the magnitude of the drought severity is greater in Agouim than in Mansour Eddahbi Dam.

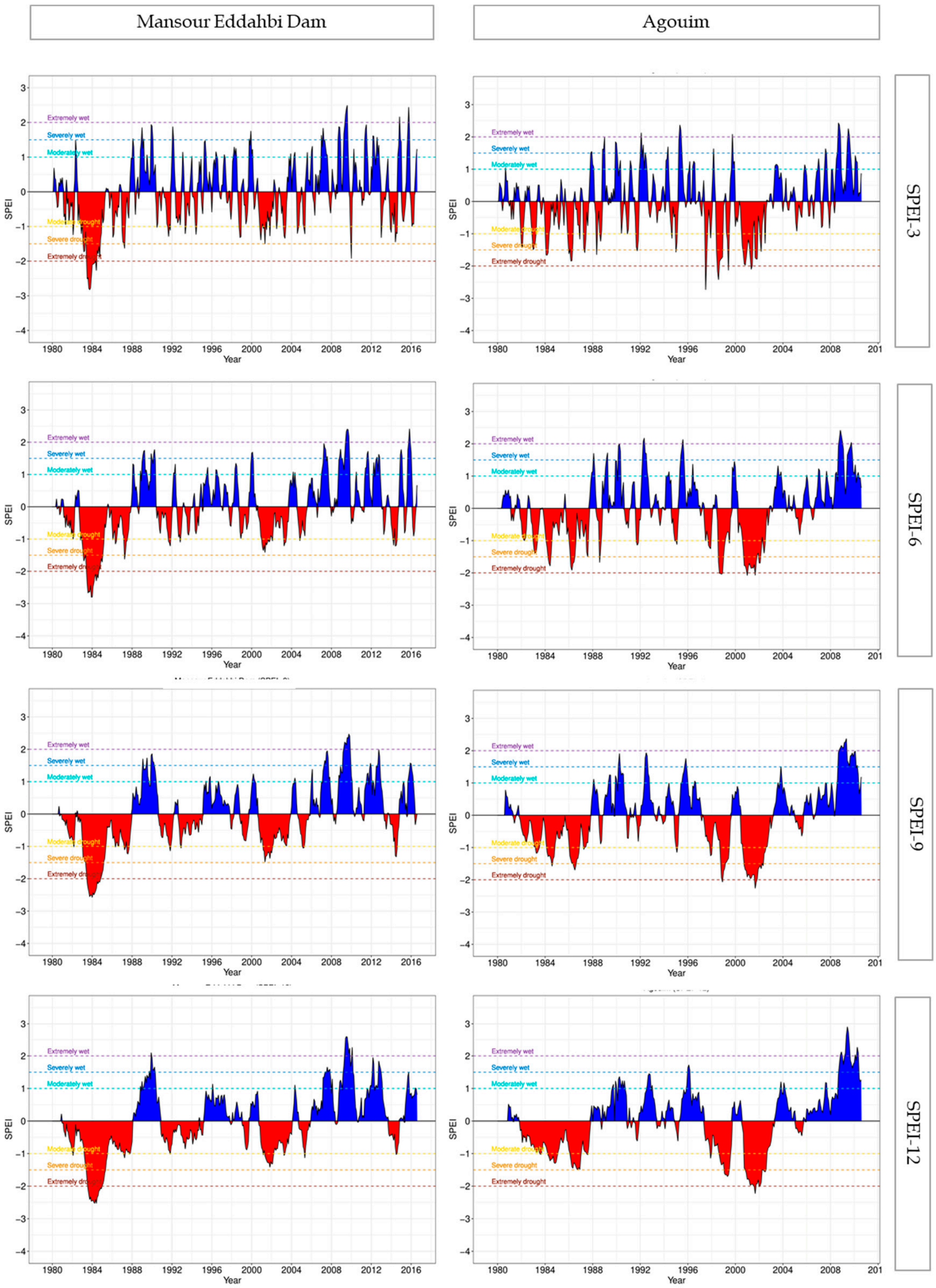

Figure 7. Temporal evolution of SPEI values showing wet and dry periods at 3-, 6-, 9-, and 12-month timescales. Red and blue represent dry and wet periods, respectively.

Table 4 summarizes drought characteristics, including the duration, severity, and intensity for the SPI and SPEI indices at various temporal scales (3-,6-,9-, and 12-). The results reveal that the duration of dry and wet events increased as the timescale of the indices increased for all the meteorological stations considered. The results also indicate that drought frequency was low (<19%) across all the timescales considered for both SPI and SPEI. Mansour Eddahbi Dam and Assaka showed the highest frequency for SPI-3 and SPEI-3, respectively. This indicates that the impact of temperature of drought tends to be larger in Assaka compared to Mansour Eddahbi Dam. Table 4 also reveals that the drought's average duration and intensity increased as the timescale increased for both the SPI and SPEI, showing that the drought became prolonged.

Table 4. Characterization of duration, frequency, and intensity for dry events from SPI and SPEI.

		SPI				SPEI		
		Duration	**Frequency**	**Intensity**		**Duration**	**Frequency**	**Intensity**
Mansour Eddahbi Dam	SPI-3	2.00	16.67	−1.46	SPEI-3	2.63	14.32	−1.51
	SPI-6	3.89	15.77	−1.65	SPEI-6	4.21	13.41	−1.55
	SPI-9	5.33	14.41	−1.84	SPEI-9	5.40	12.27	−1.60
	SPI-12	6.33	12.84	−1.94	SPEI-12	4.80	10.91	−1.66
Agouim	SPI-3	1.77	15.54	−1.50	SPEI-3	2.85	15.49	−1.56
	SPI-6	3.19	15.09	−1.63	SPEI-6	4.13	16.85	−1.48
	SPI-9	6.08	16.44	−1.61	SPEI-9	7.25	15.76	−1.51
	SPI-12	9.63	17.34	−1.61	SPEI-12	8.71	16.58	−1.47
Agouilal	SPI-3	1.97	15.54	−1.44	SPEI-3	3.10	14.77	−1.54
	SPI-6	3.83	15.54	−1.68	SPEI-6	3.48	16.59	−1.49
	SPI-9	4.47	17.12	−1.69	SPEI-9	6.83	18.64	−1.44
	SPI-12	7.36	18.24	−1.67	SPEI-12	7.60	17.27	−1.49
M'semrir	SPI-3	1.70	14.19	−1.58	SPEI-3	2.26	15.91	−1.45
	SPI-6	3.39	13.74	−1.44	SPEI-6	4.27	14.55	−1.49
	SPI-9	3.30	14.86	−1.49	SPEI-9	6.09	15.23	−1.49
	SPI-12	4.62	13.51	−1.57	SPEI-12	6.00	15.00	−1.52
Assaka	SPI-3	1.97	10.14	−1.31	SPEI-3	2.81	18.27	−1.41
	SPI-6	3.94	14.19	−1.46	SPEI-6	3.71	18.75	−1.38
	SPI-9	5.21	16.44	−1.51	SPEI-9	4.93	17.79	−1.36
	SPI-12	8.20	18.47	−1.53	SPEI-12	5.93	19.95	−1.33
Ifre	SPI-3	1.71	11.94	−1.30	SPEI-3	2.21	14.09	−1.52
	SPI-6	4.00	16.22	−1.50	SPEI-6	4.44	16.14	−1.45
	SPI-9	6.09	15.09	−1.67	SPEI-9	5.14	16.36	−1.49
	SPI-12	6.60	14.86	−1.60	SPEI-12	9.75	17.73	−1.47
Ait Mouted	SPI-3	1.86	15.54	−1.55	SPEI-3	3.17	17.55	−1.43
	SPI-6	3.75	16.89	-1.61	SPEI-6	3.59	18.99	−1.41
	SPI-9	3.82	14.64	−1.65	SPEI-9	5.92	17.07	−1.49
	SPI-12	7.30	16.44	−1.51	SPEI-12	7.11	15.38	−1.54

Figure 8 shows the temporal evolution of different drought classes for the SPI and SPEI, as categorized in Table 1. The results show severe drought in 1981–1984, 2000–2001, and 2013–2014, with 2001 being the driest year during the study period. Over 75% of both SPEI and SPI values returned drought during this period. The results show moderate and mild drought was the dominant drought category for any dry year. Conversely, wet years were experienced in 1988–1990 and 2007–2010, with 1989 being the wettest year.

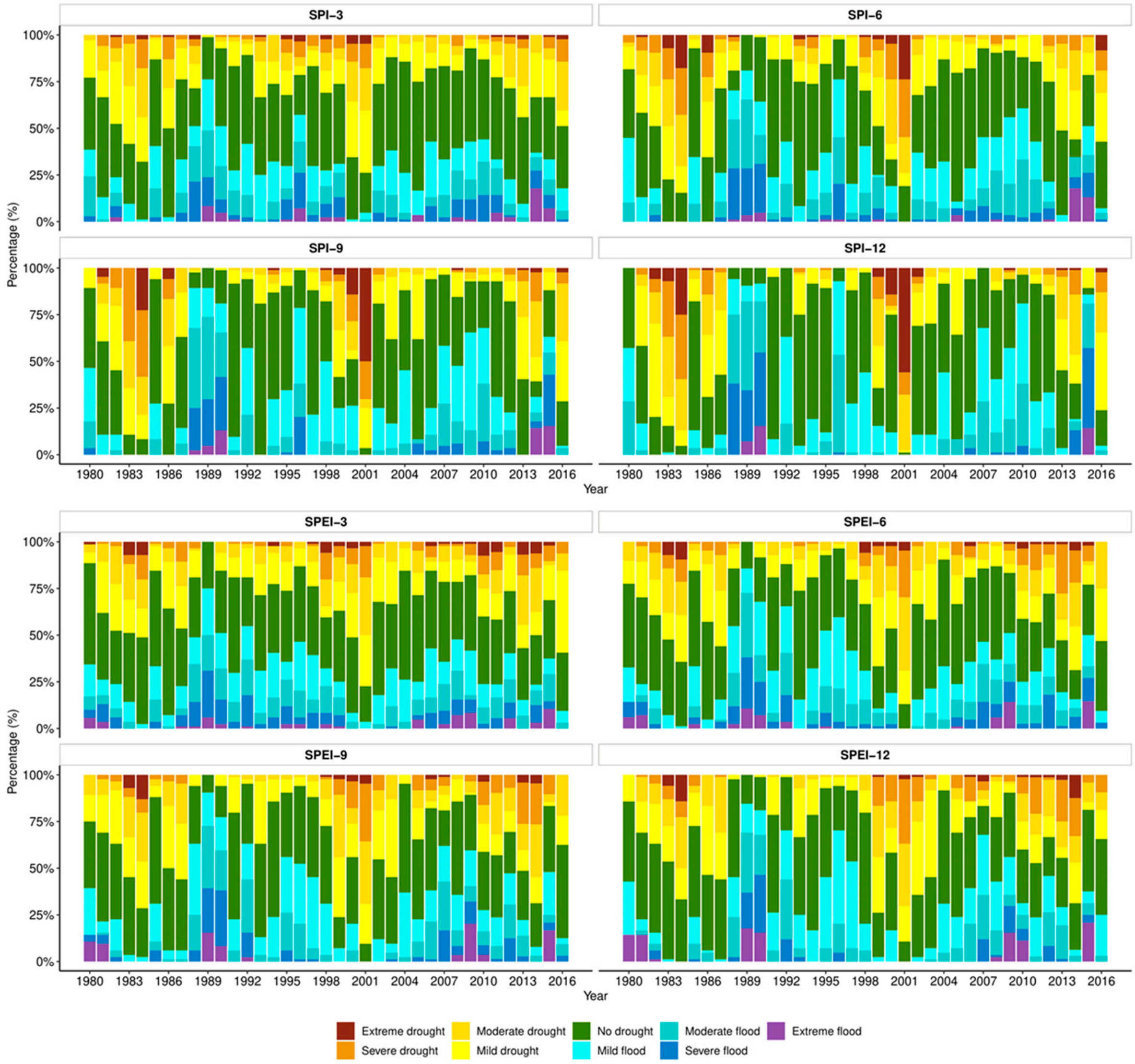

Figure 8. SPI/SPEI category's percentage in the UDB.

4. Conclusions

This study examined historical temperature and precipitation data to explore their temporal patterns and trends. The results reveal changes in temperature and precipitation distributions. The climate variability of the UDB has been assessed using temperature and rainfall time series. Various tests were performed to accomplish this, including Descriptive Statistics, Mann–Kendall's, and Sen's Slope tests. Overall, our results demonstrate that the annual trends of maximum and minimum temperature are more visible than for precipitation. In addition, the monthly trend analysis produced a mix of statistically significant and insignificant upward and downward trends. The monthly increasing trend is generally more noticeable for maximum temperature than minimum temperature.

However, precipitation increased in Ifre and Ait Mouted during September, with a decrease in January and April for Assaka. No statistically significant monthly trend was detected at Mansour Eddahbi Dam, M'semrir, Agouim, or Agouilal. The area has inherited a heterogeneous meteorological situation and climate variability over the study period. Several dry years were experienced in the UDB. According to SPI and SPEI analysis, the UDB has experienced several severe drought conditions. As a result, these findings provide several important insights into climate variability and change based on rainfall and temperature data over the UDB's seven meteorological stations. No significant annual trend was detected for rainfall. Our results revealed that temperatures and precipitation vary significantly in space and time in the UDB.

Water scarcity is the major problem in arid and semi-arid regions [72,73] and in the UDB [51,74]. Against the backdrop of global warming, the results illustrated that Tmax showed a significant positive trend for the stations considered, except the Mansour Eddahbi Dam. Such an increase may have contributed to the observed reduction in water availability experienced in the region due to increased evaporation. The UDB population's stability is closely associated with watercourses. Therefore, the high variability recorded in the study has led the portion of the population that relies on agriculture for their livelihood to move close to rivers. Given the arid and semi-arid climate of the region, the Draa and Dadès rivers serve as the primary lifelines. Moreover, the temporal evolution of the drought category shows a decadal pattern of negative SPI and SPEI values. Drying periods were observed in the early 1980s, 1990s, and 2000s, while wetting periods were observed in the late 1980s, mid-1990s, and late 2000s. Studies have reported linkages between drought in Morocco and the North Atlantic Oscillation (NAO). For instance, Xoplaki [75] attributed the drying conditions since the late 1970s over the Mediterranean region to the positive phase of NAO. Conversely, the negative phase of NAO has been linked with precipitation anomalies especially during the boreal winter season over the Atlantic coast of Morocco [76,77].

Such analyses provided in this paper are essential for developing effective mitigation and adaptation strategies that address both the immediate and long-term challenges of changing patterns and drought. By recognizing the complex interplay of factors, societies can work towards sustainable development that conserves natural resources while supporting livelihoods. In addition to more efficient water use practices, new alternatives to respond to the growing demands of water in the UDB should be considered: (i) water management planning cognizant of interannual and interdecadal climate variability; (ii) long-term water planning. It is critical that policy makers, researchers, and communities work together to develop comprehensive adaptation and mitigation strategies that address the unique vulnerabilities of oasis agriculture in the face of climate change.

Author Contributions: Conceptualization, F.E.Q., S.A. and M.Y.K.; methodology, F.E.Q., S.A., O.A.O. and M.Y.K.; writing—original draft preparation, F.E.Q., O.A.O. and S.A.; writing—review and editing, F.E.Q., Q.B.P., S.A., A.K. and O.A.O.; supervision, M.Y.K. and S.A.; Data Curation, F.E.Q.; Formal Analysis, F.E.Q. and S.A.; Investigation, F.E.Q.; Software, F.E.Q. and S.A.; Visualization, F.E.Q., Q.B.P., S.A., A.K. and O.A.O.; Validation, F.E.Q., S.A., O.A.O. and M.Y.K. All authors have read and agreed to the published version of the manuscript.

Funding: There is no external funding for this work.

Data Availability Statement: Data set available on request to corresponding authors.

Conflicts of Interest: The authors declare no conflict of interest.

Appendix A

Table A1. Mann–Kendall Test and Sen's Slope estimator for monthly rainfall.

Mansour Eddahbi Dam	Mann–Kendall Test				Sen's Slope	M'semrir	Mann–Kendall Test				Sen's Slope
	Z	Kendall's Tau	*p*-Value	Trend			Z	Kendall's Tau	*p*-Value	Trend	
January	−0.96	−0.12	0.34	No trend	0.00	January	−1.38	−0.16	0.17	No trend	−0.20
February	−1.07	−0.13	0.29	No trend	−0.01	February	−0.47	−0.06	0.64	No trend	−0.07
March	−0.14	−0.02	0.89	No trend	0.00	Mars	1.35	0.16	0.18	No trend	0.41
April	0.74	0.09	0.46	No trend	0.00	April	−0.68	−0.08	0.50	No trend	−0.06
May	−0.72	−0.09	0.47	No trend	0.00	May	−0.18	−0.02	0.85	No trend	−0.03
June	0.59	0.07	0.56	No trend	0.00	June	0.18	0.02	0.85	No trend	0.02
July	1.02	0.13	0.31	No trend	0.00	July	1.79	0.21	0.07	No trend	0.10
August	1.78	0.21	0.08	No trend	0.18	August	0.73	0.09	0.46	No trend	0.20
September	1.01	0.12	0.31	No trend	0.16	September	1.77	0.20	0.08	No trend	0.63
October	1.27	0.15	0.20	No trend	0.12	October	0.60	0.07	0.55	No trend	0.18
November	−0.89	−0.11	0.37	No trend	0.00	November	−0.17	−0.02	0.86	No trend	−0.01
December	−0.15	−0.02	0.88	No trend	0.00	December	−0.75	−0.09	0.45	No trend	−0.08

Table A1. *Cont.*

Assaka	Mann–Kendall Test				Sen's Slope
	Z	Kendall's Tau	*p*-Value	Trend	
January	**−2.55**	**−0.31**	0.01 *	**Trend detected**	**−0.07**
February	−1.50	−0.18	0.13	No trend	−0.03
Mars	−0.20	−0.02	0.84	No trend	0.00
April	**−2.12**	**−0.26**	0.03 *	**Trend detected**	**0.00**
May	−1.69	−0.21	0.09	No trend	0.00
June	−0.69	−0.09	0.49	No trend	0.00
July	−0.85	−0.11	0.40	No trend	0.00
August	0.04	0.01	0.97	No trend	0.00
September	1.52	0.18	0.13	No trend	0.20
October	0.16	0.02	0.87	No trend	0.00
November	−1.40	−0.17	0.16	No trend	−0.05
December	−0.43	−0.05	0.67	No trend	0.00

Ifre	Mann–Kendall Test				Sen's Slope
	Z	Kendall's Tau	*p*-Value	Trend	
January	−0.86	−0.11	0.39	No trend	0.00
February	−0.86	−0.10	0.39	No trend	0.00
Mars	0.67	0.08	0.50	No trend	0.11
April	−0.24	−0.03	0.81	No trend	0.00
May	−0.94	−0.12	0.35	No trend	0.00
June	0.44	0.06	0.66	No trend	0.00
July	−0.07	−0.01	0.95	No trend	0.00
August	−0.56	−0.07	0.57	No trend	0.00
September	**2.31**	**0.28**	0.02 *	**Trend detected**	**0.37**
October	1.16	0.14	0.25	No trend	0.20
November	−0.25	−0.03	0.80	No trend	0.00
December	−0.79	−0.10	0.43	No trend	0.00

Agouim	Mann–Kendall Test				Sen's Slope
	Z	Kendall's Tau	*p*-Value	Trend	
January	−0.55	−0.06	0.58	No trend	−0.12
February	−0.87	−0.10	0.39	No trend	−0.30
Mars	−0.56	−0.07	0.57	No trend	−0.19
April	0.53	0.07	0.59	No trend	0.00
May	0.28	0.03	0.78	No trend	0.00
June	1.37	0.17	0.17	No trend	0.00
July	1.63	0.19	0.10	No trend	0.06
August	1.83	0.22	0.07	No trend	0.23
September	1.06	0.12	0.29	No trend	0.20
October	0.43	0.05	0.67	No trend	0.10
November	−0.49	−0.06	0.63	No trend	−0.12
December	−0.81	−0.10	0.42	No trend	−0.07

Ait Mouted	Mann–Kendall Test				Sen's Slope
	Z	Kendall's Tau	*p*-Value	Trend	
January	−0.84	−0.10	0.40	No trend	−0.03
February	−0.49	−0.06	0.63	No trend	−0.01
Mars	0.98	0.11	0.33	No trend	0.20
April	−0.88	−0.11	0.38	No trend	−0.05
May	0.34	0.04	0.73	No trend	0.00
June	−0.16	−0.02	0.87	No trend	0.00
July	0.97	0.12	0.33	No trend	0.00
August	0.88	0.10	0.38	No trend	0.05
September	**2.32**	**0.27**	0.02 *	**Trend detected**	**0.49**
October	1.37	0.16	0.17	No trend	0.31
November	−0.04	−0.01	0.97	No trend	0.00
December	−0.87	−0.10	0.38	No trend	−0.07

Agouilal	Mann–Kendall Test				Sen's Slope
	Z	Kendall's Tau	*p*-Value	Trend	
January	−1.15	−0.14	0.25	No trend	0.00
February	−1.04	−0.13	0.30	No trend	−0.03
Mars	0.00	0.00	1.00	No trend	0.00
April	0.46	0.06	0.64	No trend	0.00
May	−0.58	−0.07	0.56	No trend	0.00
June	−0.01	0.00	0.99	No trend	0.00
July	0.29	0.04	0.77	No trend	0.00
August	0.38	0.05	0.70	No trend	0.04
September	1.54	0.18	0.12	No trend	0.25
October	0.41	0.05	0.68	No trend	0.02
November	−1.20	−0.15	0.23	No trend	−0.03
December	−0.45	−0.06	0.65	No trend	0.00

Note: * Indicates $p < 0.05$. Bold values are significative at 95% family-wise confidence level. $p < 0.05$ im-plies a monotonic trend, positive Z signifies an increase, and negative Z indicates a decrease.

Table A2. Mann–Kendall Test and Sen's Slope estimator for Tmin.

Mansour Eddahbi Dam	Mann–Kendall Test				Sen's Slope
	Z	Kendall's Tau	*p*-Value	Trend	
January	3.17	**0.37**	0.002 *	**Trend detected**	0.10
February	1.60	0.19	0.11	No trend	0.05
Mars	**2.34**	**0.27**	0.02 *	**Trend detected**	**0.09**
April	**2.74**	**0.32**	0.006 *	**Trend detected**	**0.10**
May	**2.95**	**0.34**	0.003 *	**Trend detected**	**0.14**
June	**2.91**	**0.34**	0.003 *	**Trend detected**	**0.14**
July	**3.56**	**0.43**	0.0004 *	**Trend detected**	**0.16**
August	**3.39**	**0.39**	0.0007 *	**Trend detected**	**0.12**
September	**2.87**	**0.33**	0.004 *	**Trend detected**	**0.10**
October	**2.82**	**0.34**	0.005 *	**Trend detected**	**0.13**
November	1.71	0.21	0.09	No trend	0.06
December	**2.28**	**0.27**	0.02*	**Trend detected**	**0.06**

M'semrir	Mann–Kendall Test				Sen's Slope
	Z	Kendall's Tau	*p*-Value	Trend	
January	1.48	0.18	0.14	No trend	0.03
February	−0.90	−0.11	0.37	No trend	−0.04
Mars	−0.76	−0.09	0.45	No trend	−0.03
April	0.29	0.04	0.77	No trend	0.01
May	−0.34	−0.04	0.73	No trend	−0.01
June	1.94	0.23	0.05	No trend	0.04
July	1.20	0.14	0.23	No trend	0.02
August	−0.04	−0.01	0.97	No trend	0.00
September	−0.16	−0.02	0.88	No trend	0.00
October	0.07	0.01	0.94	No trend	0.00
November	−0.16	−0.02	0.88	No trend	0.00
December	−0.87	−0.11	0.39	No trend	−0.03

Table A2. *Cont.*

Assaka	Mann–Kendall Test				Sen's Slope	Ifre	Mann–Kendall Test				Sen's Slope
	Z	Kendall's Tau	p-Value	Trend			Z	Kendall's Tau	p-Value	Trend	
January	**3.63**	**0.43**	0.0003 *	**Trend detected**	**0.11**	January	1.52	0.18	0.13	No trend	0.05
February	1.50	0.18	0.13	No trend	0.04	February	−1.44	−0.17	0.15	No trend	−0.06
Mars	1.42	0.17	0.16	No trend	0.04	Mars	−0.63	−0.07	0.53	No trend	−0.02
April	**3.25**	**0.38**	0.001 *	**Trend detected**	**0.14**	April	1.26	0.15	0.21	No trend	0.03
May	**4.09**	**0.48**	0.00 *	**Trend detected**	**0.18**	May	−0.17	−0.02	0.86	No trend	0.00
June	**3.33**	**0.40**	0.0009 *	**Trend detected**	**0.16**	June	1.23	0.14	0.22	No trend	0.06
July	**4.42**	**0.53**	0.00 *	**Trend detected**	**0.17**	July	1.21	0.14	0.22	No trend	0.05
August	**2.90**	**0.35**	0.003 *	**Trend detected**	**0.14**	August	1.95	0.23	0.05	No trend	0.09
September	−0.07	−0.01	0.94	No trend	0.00	September	−0.01	0.00	0.99	No trend	0.00
October	−0.07	−0.01	0.94	No trend	0.00	October	1.10	0.13	0.27	No trend	0.05
November	**2.62**	**0.31**	0.009 *	**Trend detected**	**0.08**	November	−0.31	−0.04	0.75	No trend	−0.01
December	**3.39**	**0.41**	0.0007 *	**Trend detected**	**0.09**	December	1.06	0.13	0.29	No trend	0.04

Agouim	Mann–Kendall Test				Sen's Slope	Ait Mouted	Mann–Kendall test				Sen's Slope
	Z	Kendall's Tau	p-Value	Trend			Z	Kendall's Tau	p-Value	Trend	
January	1.94	0.25	0.05	No trend	0.07	January	−0.31	−0.04	0.76	No trend	−0.02
February	2.37	**0.30**	0.01 *	**Trend detected**	0.08	February	−0.06	−0.01	0.95	No trend	0.00
Mars	1.63	0.21	0.10	No trend	0.04	Mars	0.28	0.04	0.78	No trend	0.01
April	−0.37	−0.05	0.71	No trend	−0.02	April	1.53	0.19	0.13	No trend	0.08
May	0.54	0.07	0.59	No trend	0.04	May	1.35	0.17	0.18	No trend	0.06
June	0.39	0.05	0.70	No trend	0.02	June	0.76	0.09	0.45	No trend	0.03
July	**2.08**	**0.27**	0.037 *	**Trend detected**	**0.09**	July	1.23	0.15	0.22	No trend	0.04
August	0.37	0.05	0.71	No Trend	0.01	August	1.08	0.13	0.28	No trend	0.08
September	−0.87	−0.11	0.39	No Trend	−0.04	September	−1.24	−0.16	0.21	No trend	−0.05
October	−0.53	−0.07	0.60	No Trend	−0.03	October	0.37	0.05	0.71	No trend	0.01
November	1.09	0.14	0.28	No Trend	0.05	November	−0.37	−0.05	0.71	No trend	−0.01
December	1.23	0.16	0.22	No Trend	0.04	December	0.14	0.02	0.89	No trend	0.00

Agouilal	Mann–Kendall Test				Sen's Slope
	Z	Kendall's Tau	p-Value	Trend	
January	1.28	0.15	0.20	No trend	0.04
February	1.68	0.20	0.09	No trend	0.06
Mars	1.15	0.14	0.25	No trend	0.02
April	**2.38**	**0.29**	0.017 *	**Trend detected**	**0.06**
May	**2.04**	**0.24**	0.041 *	**Trend detected**	**0.06**
June	**3.82**	**0.45**	0.0001 *	**Trend detected**	**0.10**
July	3.98	0.47	0.07	No trend	0.10
August	**4.13**	**0.48**	0.036 *	**Trend detected**	**0.12**
September	**2.48**	**0.30**	0.013 *	**Trend detected**	**0.06**
October	**2.57**	**0.30**	0.01 *	**Trend detected**	**0.09**
November	0.30	0.04	0.77	No trend	0.00
December	1.95	0.24	0.05	No trend	0.08

Note: * Indicates $p < 0.05$. Bold values are significative at 95% family-wise confidence level. $p < 0.05$ implies a monotonic trend, positive Z signifies an increase, and negative Z indicates a decrease.

Table A3. Mann–Kendall Test and Sen's Slope estimator for Tmax.

Mansour Eddahbi Dam	Mann–Kendall Test				Sen's Slope	M'semrir	Mann–Kendall Test				
	Z	Kendall's Tau	p-Value	Trend			Z	Kendall's Tau	p-Value	Trend	Sen's Slope
January	0.45	0.05	0.66	No trend	0.02	January	1.74	0.20	0.08	No trend	0.06
February	−1.62	−0.19	0.10	No trend	−0.07	February	−0.12	−0.02	0.91	No trend	0.00
Mars	−0.25	−0.03	0.80	No trend	−0.01	Mars	0.13	0.02	0.90	No trend	0.00
April	1.61	0.19	0.11	No trend	0.04	April	**2.35**	**0.28**	0.018 *	**Trend detected**	**0.07**
May	0.31	0.04	0.75	No trend	0.00	May	**2.05**	**0.24**	0.0408 *	**Trend detected**	**0.06**
June	0.00	0.00	1.00	No trend	0.00	June	**2.22**	**0.26**	0.026 *	**Trend detected**	**0.04**
July	0.64	0.08	0.52	No trend	0.01	July	**3.48**	**0.42**	0.0005 *	**Trend detected**	**0.05**
August	0.22	0.03	0.82	No trend	0.00	August	**3.13**	**0.38**	0.0017 *	**Trend detected**	**0.05**
September	−1.28	−0.15	0.20	No trend	−0.02	September	0.84	0.10	0.40	No trend	0.01
October	0.80	0.10	0.43	No trend	0.02	October	1.69	0.21	0.09	No trend	0.05
November	0.17	0.02	0.86	No trend	0.00	November	1.23	0.15	0.22	No trend	0.04
December	−0.53	−0.06	0.60	No trend	−0.03	December	1.03	0.13	0.30	No trend	0.03

Table A3. *Cont.*

Assaka	Mann–Kendall Test Z	Kendall's Tau	p-Value	Trend	Sen's Slope	Ifre	Mann–Kendall Test Z	Kendall's Tau	p-Value	Trend	Sen's Slope
January	**−3.09**	**−0.36**	0.002 *	**Trend detected**	**−0.13**	January	**2.62**	**0.31**	0.008 *	**Trend detected**	**0.13**
February	−1.64	−0.19	0.10	No trend	−0.07	February	1.32	0.15	0.19	No trend	0.08
Mars	0.52	0.06	0.60	No trend	0.02	Mars	**2.93**	**0.34**	0.003 *	**Trend detected**	**0.10**
April	1.05	0.13	0.29	No trend	0.05	April	**3.12**	**0.36**	0.0018 *	**Trend detected**	**0.12**
May	1.38	0.16	0.17	No trend	0.05	May	**3.11**	**0.36**	0.0019 *	**Trend detected**	**0.10**
June	0.38	0.05	0.70	No trend	0.01	June	**2.40**	**0.28**	0.0164 *	**Trend detected**	**0.05**
July	1.67	0.20	0.10	No trend	0.03	July	**3.72**	**0.44**	0.0002 *	**Trend detected**	**0.07**
August	−1.34	−0.16	0.18	No trend	−0.02	August	**3.09**	**0.37**	0.0020 *	**Trend detected**	**0.05**
September	−0.90	−0.11	0.37	No trend	−0.03	September	**2.16**	**0.26**	0.03 *	**Trend detected**	**0.07**
October	−0.27	−0.03	0.79	No trend	−0.01	October	**3.17**	**0.37**	0.001 *	**Trend detected**	**0.10**
November	0.54	0.07	0.59	No trend	0.02	November	**2.22**	**0.26**	0.026 *	**Trend detected**	**0.09**
December	**−3.80**	**−0.46**	0.0001 *	**Trend detected**	**−0.14**	December	**2.76**	**0.33**	0.006 *	**Trend detected**	**0.10**
Agouim	**Z**	**Kendall's Tau**	**p-Value**	**Trend**	**Sen's Slope**	**Ait Mouted**	**Z**	**Kendall's Tau**	**p-Value**	**Trend**	**Sen's Slope**
January	**−2.35**	**−0.3**	0.019 *	**Trend detected**	**−0.15**	January	1.09	0.13	0.28	No trend	0.07
February	−1.94	−0.25	0.05	No trend	−0.15	February	0.64	0.08	0.52	No trend	0.03
Mars	**−2.4**	**−0.31**	0.016 *	**Trend detected**	**−0.24**	Mars	**2.29**	**0.27**	0.0221 *	**Trend detected**	**0.1**
April	−1.02	−0.13	0.31	No trend	−0.06	April	**2.94**	**0.36**	0.0033 *	**Trend detected**	**0.09**
May	−0.99	−0.13	0.32	No trend	−0.05	May	**3.44**	**0.41**	0.0006 *	**Trend detected**	**0.14**
June	**−1.84**	**−0.24**	0.07	**Trend detected**	**−0.08**	June	**3.3**	**0.4**	0.0001 *	**Trend detected**	**0.14**
July	−1.55	−0.2	0.12	No trend	−0.04	July	**4.17**	**0.5**	0.0000 *	**Trend detected**	**0.14**
August	−1.43	−0.18	0.15	No trend	−0.04	August	**3.56**	**0.43**	0.0004 *	**Trend detected**	**0.11**
September	**−2.14**	**−0.27**	0.032 *	**Trend detected**	**−0.07**	September	**3.59**	**0.43**	0.0003 *	**Trend detected**	**0.14**
October	0.81	0.11	0.42	No trend	0	October	**2.48**	**0.3**	0.0133 *	**Trend detected**	**0.1**
November	−0.26	−0.03	0.8	No trend	−0.01	November	**3.51**	**0.42**	0.0004 *	**Trend detected**	**0.14**
December	−0.44	−0.06	0.66	No trend	−0.02	December	1.44	0.18	0.15	No trend	0.07
Agouilal	**Z**	**Kendall's Tau**	**p-Value**	**Trend**	**Sen's Slope**						
January	0.38	0.05	0.70	No trend	0.01						
February	1.37	0.16	0.17	No trend	0.06						
Mars	1.31	0.15	0.19	No trend	0.05						
April	**2.82**	**0.33**	0.005 *	**Trend detected**	**0.13**						
May	**2.95**	**0.34**	0.003 *	**Trend detected**	**0.11**						
June	**3.43**	**0.40**	0.0006 *	**Trend detected**	**0.09**						
July	**4.86**	**0.56**	0.00 *	**Trend detected**	**0.12**						
August	**4.61**	**0.53**	0.00 *	**Trend detected**	**0.13**						
September	**2.87**	**0.34**	0.004 *	**Trend detected**	**0.07**						
October	**3.35**	**0.39**	0.0008 *	**Trend detected**	**0.10**						
November	**3.25**	**0.38**	0.001 *	**Trend detected**	**0.12**						
December	−1.20	−0.14	0.23	No trend	−0.03						

Note: * Indicates $p < 0.05$. Bold values are significative at 95% family-wise confidence level. $p < 0.05$ implies a monotonic trend, positive Z signifies an increase, and negative Z indicates a decrease.

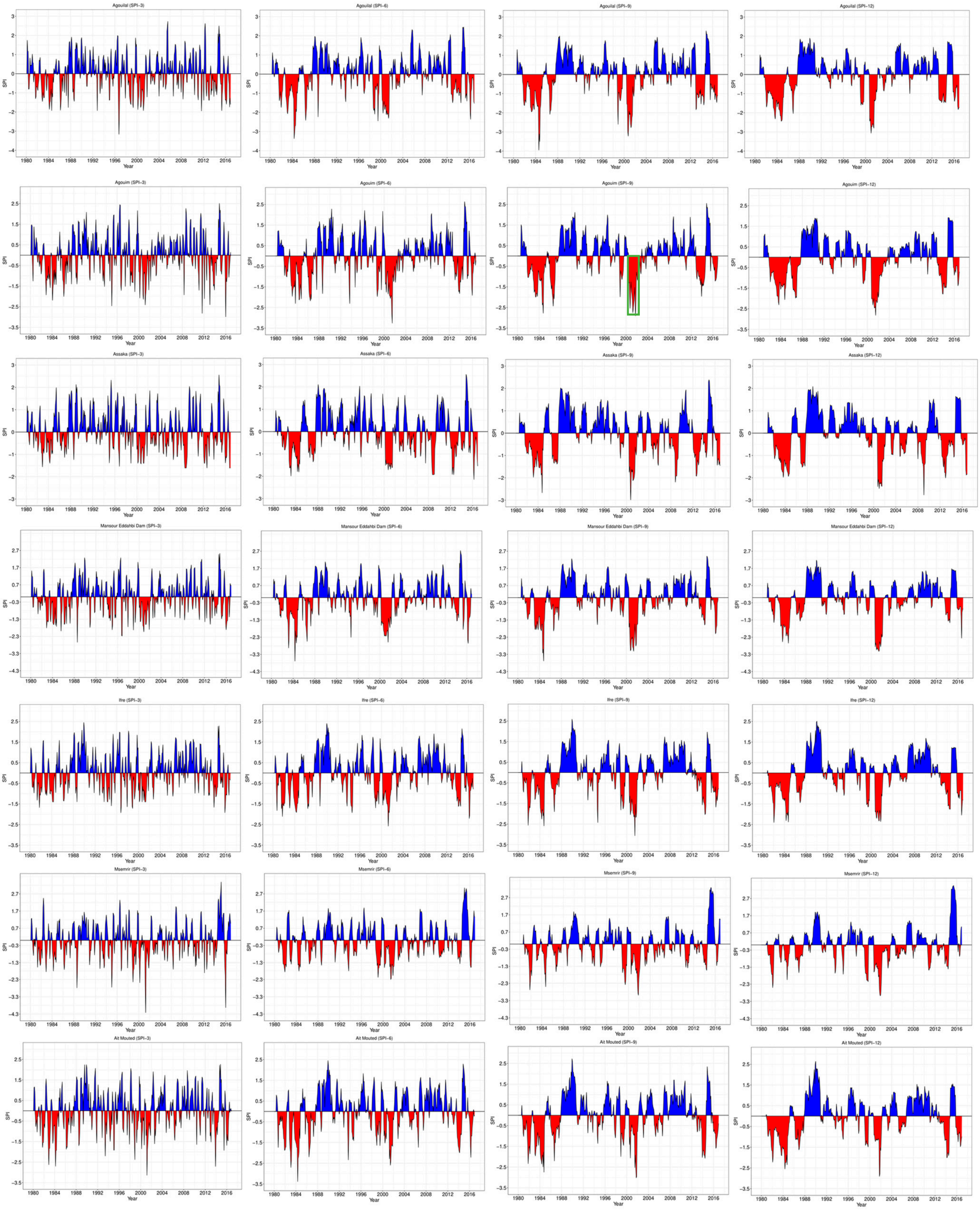

Figure A1. Temporal evolution of SPI values showing wet and dry periods at 3-, 6-, 9-, and 12-month timescales for the seven meteorological stations. Red and blue represent dry and wet periods, respectively.

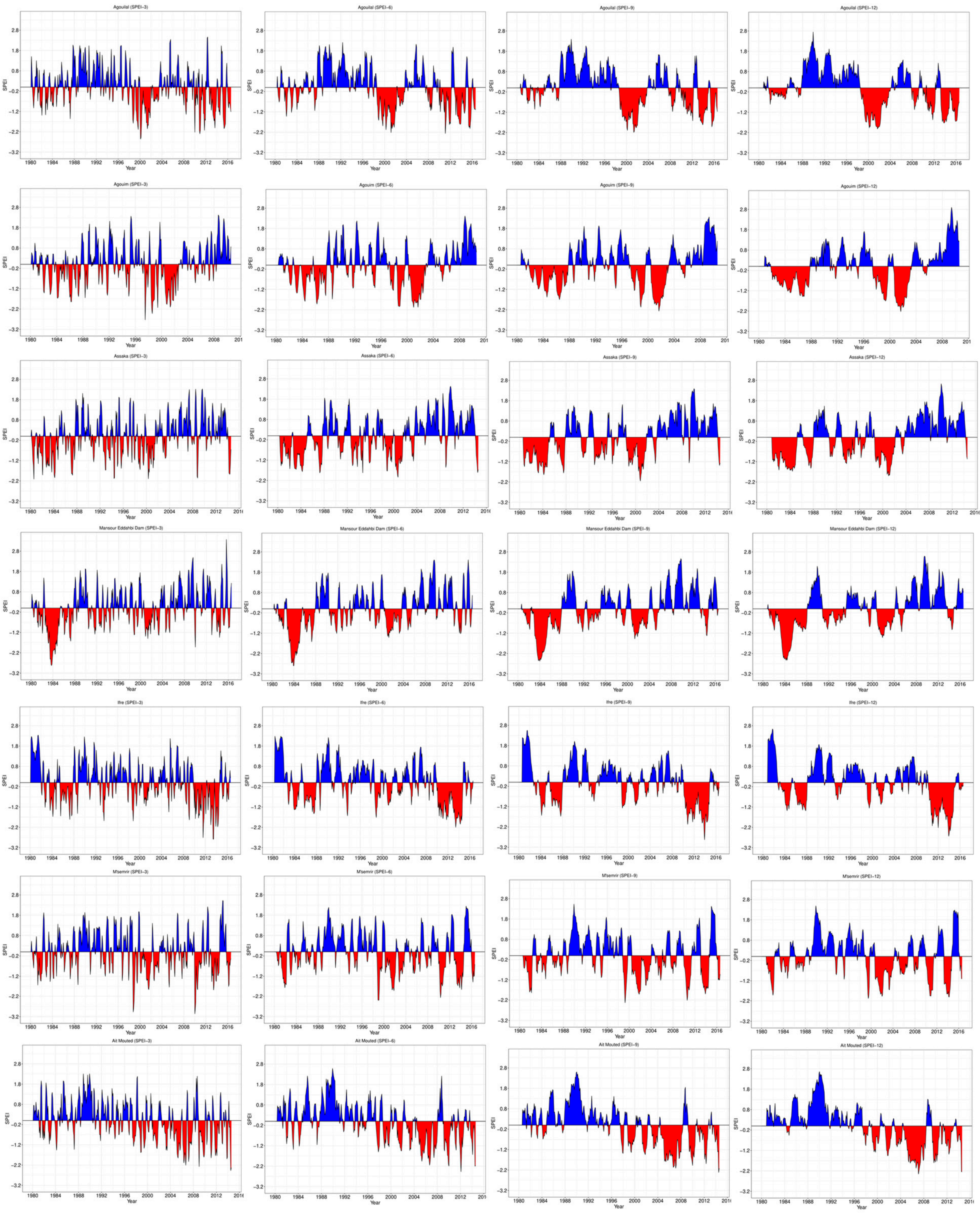

Figure A2. Temporal evolution of SPEI values showing wet and dry periods at 3-, 6-, 9-, and 12-month timescales for the seven meteorological stations. Red and blue represent dry and wet periods, respectively.

References

1. Guan, X.; Zang, Y.; Meng, Y.; Liu, Y.; Lv, H.; Yan, D. Study on Spatiotemporal Distribution Characteristics of Flood and Drought Disaster Impacts on Agriculture in China. *Int. J. Disaster Risk Reduct.* **2021**, *64*, 102504. [CrossRef]
2. Van der Wiel, K.; Bintanja, R. Contribution of Climatic Changes in Mean and Variability to Monthly Temperature and Precipitation Extremes. *Commun. Earth Environ.* **2021**, *2*, 1. [CrossRef]
3. Almazroui, M.; Saeed, F.; Islam, M.N.; Alkhalaf, A.K. Assessing the Robustness and Uncertainties of Projected Changes in Temperature and Precipitation in AR4 Global Climate Models over the Arabian Peninsula. *Atmos. Res.* **2016**, *182*, 163–175. [CrossRef]
4. Sa'adi, Z.; Shahid, S.; Chung, E.S.; bin Ismail, T. Projection of Spatial and Temporal Changes of Rainfall in Sarawak of Borneo Island Using Statistical Downscaling of CMIP5 Models. *Atmos. Res.* **2017**, *197*, 446–460. [CrossRef]
5. Sung, J.H.; Chung, E.S.; Kim, Y.; Lee, B.R. Meteorological Hazard Assessment Based on Trends and Abrupt Changes in Rainfall Characteristics on the Korean Peninsula. *Theor. Appl. Climatol.* **2017**, *127*, 305–326. [CrossRef]
6. Pour, S.H.; Shahid, S.; Chung, E.S.; Wang, X.J. Model Output Statistics Downscaling Using Support Vector Machine for the Projection of Spatial and Temporal Changes in Rainfall of Bangladesh. *Atmos. Res.* **2018**, *213*, 149–162. [CrossRef]
7. Zahabiyoun, B.; Goodarzi, M.R.; Bavani, A.R.M.; Azamathulla, H.M. Assessment of Climate Change Impact on the Gharesou River Basin Using SWAT Hydrological Model. *Clean—Soil Air Water* **2013**, *41*, 601–609. [CrossRef]
8. Sung, J.H.; Chung, E.S. Development of Streamflow Drought Severity–Duration–Frequency Curves Using the Threshold Level Method. *Hydrol. Earth Syst. Sci.* **2014**, *18*, 3341–3351. [CrossRef]
9. Mohsenipour, M.; Shahid, S.; Chung, E.-S.; Wang, X.-J. Changing Pattern of Droughts during Cropping Seasons of Bangladesh. *Water Resour. Manag.* **2018**, *32*, 1555–1568. [CrossRef]
10. Ahmed, K.; Shahid, S.; bin Harun, S.; Wang, X.J. Characterization of Seasonal Droughts in Balochistan Province, Pakistan. *Stoch. Environ. Res. Risk Assess.* **2016**, *30*, 747–762. [CrossRef]
11. Chevuturi, A.; Klingaman, N.P.; Turner, A.G.; Guo, L.; Vidale, P.L. Projected Changes in the East Asian Hydrological Cycle for Different Levels of Future Global Warming. *Atmosphere* **2022**, *13*, 405. [CrossRef]
12. Montaseri, M.; Amirataee, B. Comprehensive Stochastic Assessment of Meteorological Drought Indices. *Int. J. Climatol.* **2017**, *37*, 998–1013. [CrossRef]
13. Tsatsaris, A.; Kalogeropoulos, K.; Stathopoulos, N.; Louka, P.; Tsanakas, K.; Tsesmelis, D.E.; Krassanakis, V.; Petropoulos, G.P.; Pappas, V.; Chalkias, C. Geoinformation Technologies in Support of Environmental Hazards Monitoring under Climate Change: An Extensive Review. *ISPRS Int. J. Geo-Inf.* **2021**, *10*, 94. [CrossRef]
14. Gaznayee, H.A.A.; Al-Quraishi, A.M.F.; Mahdi, K.; Messina, J.P.; Zaki, S.H.; Razvanchy, H.A.S.; Hakzi, K.; Huebner, L.; Ababakr, S.H.; Riksen, M.; et al. Drought Severity and Frequency Analysis Aided by Spectral and Meteorological Indices in the Kurdistan Region of Iraq. *Water* **2022**, *14*, 3024. [CrossRef]
15. Bhaga, T.D.; Dube, T.; Shekede, M.D.; Shoko, C. Impacts of Climate Variability and Drought on Surface Water Resources in Sub-Saharan Africa Using Remote Sensing: A Review. *Remote Sens.* **2020**, *12*, 4184. [CrossRef]
16. Sheik Mujabar, P. Spatial-Temporal Variation of Land Surface Temperature of Jubail Industrial City, Saudi Arabia Due to Seasonal Effect by Using Thermal Infrared Remote Sensor (TIRS) Satellite Data. *J. Afr. Earth Sci.* **2019**, *155*, 54–63. [CrossRef]
17. He, J.; Li, B.; Yu, Y.; Sun, L.; Zhang, H.; Malik, I.; Wistuba, M.; Yu, R. Temporal Variability of Temperature, Precipitation and Drought Indices in Hyper-Arid Region of Northwest China for the Past 60 Years. *Atmosphere* **2022**, *13*, 1561. [CrossRef]
18. Sebbar, A.; Mohammed, H.; Fougrach, H.; Badri, W. Étude Des Variations Climatiques De La Région Centre Du Maroc. *25ème Colloq. L'association Int. Climatol. Grenoble* **2012**, *2012*, 709–714.
19. Umar, D.A.; Ramli, M.F.; Aris, A.Z.; Jamil, N.R.; Aderemi, A.A. Evidence of Climate Variability from Rainfall and Temperature Fluctuations in Semi-Arid Region of the Tropics. *Atmos. Res.* **2019**, *224*, 52–64. [CrossRef]
20. Choukrani, G.; Hamimsa, A.; Said, M.E.M.; Babqiqi, A. Diagnostic et Projection Future Du Changement Climatique En Zone Aride. Cas de La Région Marrakech-Safi (Maroc). Diagnosis and Future Projection of Climate Change in Arid Zone. Case of Marrakech-Safi Region (Morocco). *Larhyss J.* **2018**, *36*, 49–63.
21. Wen, X.; Wu, X.; Gao, M. Spatiotemporal Variability of Temperature and Precipitation in Gansu Province (Northwest China) during 1951–2015. *Atmos. Res.* **2017**, *197*, 132–149. [CrossRef]
22. Hänsel, S.; Medeiros, D.M.; Matschullat, J.; Petta, R.A.; de Mendonça Silva, I. Assessing Homogeneity and Climate Variability of Temperature and Precipitation Series in the Capitals of North-Eastern Brazil. *Front. Earth Sci.* **2016**, *4*, 29. [CrossRef]
23. Acharki, S.; Amharref, M.; El Halimi, R.; Bernoussi, A.S. Assessment by Statistical Approach of Climate Change Impact on Water Resources: Application to the Gharb Perimeter (Morocco). *Rev. Sci. l'Eau* **2019**, *32*, 291–315. [CrossRef]
24. Chand, M.; Bhattarai, B.; Baral, P.; Pradhananga, N. Trend Analysis of Temperature Data for Narayani River Basin, Nepal. *Sci* **2019**, *1*, 21. [CrossRef]
25. Iqbal, M.A.; Penas, A.; Cano-Ortiz, A.; Kersebaum, K.C.; Herrero, L.; del Río, S. Analysis of Recent Changes in Maximum and Minimum Temperatures in Pakistan. *Atmos. Res.* **2016**, *168*, 234–249. [CrossRef]
26. Khomsi, K.; Mahe, G.; Sinan, M.; Snoussi, M. Hydro-Climatic Variability in Two Moroccan Basins: Comparative Analysis of Temperature, Rainfall and Runoff Regimes. *IAHS-AISH Proc. Reports* **2013**, *359*, 183–190.
27. Yao, J.; Chen, Y. Trend Analysis of Temperature and Precipitation in the Syr Darya Basin in Central Asia. *Theor. Appl. Climatol.* **2015**, *120*, 521–531. [CrossRef]

28. Archer, D.H.A. Analysis of Temperature Trends in Sutluj River Basin, India. *J. Earth Sci. Clim. Chang.* **2014**, *5*, 222. [CrossRef]
29. Dore, M.H.I. Climate Change and Changes in Global Precipitation Patterns: What Do We Know ? *Environ. Int.* **2005**, *31*, 1167–1181. [CrossRef]
30. Knippertz, P.; Christoph, M.; Speth, P. Long-Term Precipitation Variability in Morocco and the Link to the Large-Scale Circulation in Recent and Future Climates. *Meteorol. Atmos. Phys.* **2003**, *83*, 67–88. [CrossRef]
31. Xu, S.; Yu, Z.; Yang, C.; Ji, X.; Zhang, K. Trends in Evapotranspiration and Their Responses to Climate Change and Vegetation Greening over the Upper Reaches of the Yellow River Basin. *Agric. For. Meteorol.* **2018**, *263*, 118–129. [CrossRef]
32. Hartmann, D.L.; Klein Tank, M.A.M.G.; Rusticucci, M.; Alexander, L.V.; Brönnimann, S.; Charab, Y.; Dentener, F.J.; Dlugokencky, E.J.; Easterling, D.R.; Kaplan, A.; et al. Observations: Atmosphere and Surface. In *Climate Change 2013: The Physical Science Basis. Contribution of Working Group I to the Fifth Assessment Report of the Intergovernmental Panel on Climate Change*; Stocker, T.F., Qin, G.-K.D., Plattner, M., Tignor, S.K., Allen, J., Boschung, A., Nauels, Y.X., Eds.; Cambridge University Press: Cambridge, UK, 2013; Volume 44, pp. 159–254. ISBN 9781107415324.
33. Bouras, E.H.; Jarlan, L.; Er-Raki, S.; Balaghi, R.; Amazirh, A.; Richard, B.; Khabba, S. Cereal Yield Forecasting with Satellite Drought-Based Indices, Weather Data and Regional Climate Indices Using Machine Learning in Morocco. *Remote Sens.* **2021**, *13*, 3101. [CrossRef]
34. Verner, D.; Treguer, D.; Redwood, J.; Christensen, J.; McDonnell, R.; Elbert, C.; Konishi, Y.; Belghazi, S. *Climate Variability, Drought, and Drought Management in Morocco's Agricultural Sector*; World Bank Group: Washington, DC, USA, 2018.
35. Zkhiri, W.; Tramblay, Y.; Hanich, L.; Jarlan, L.; Ruelland, D. Spatiotemporal Characterization of Current and Future Droughts in the High Atlas Basins (Morocco). *Theor. Appl. Clim.* **2018**, *135*, 593–605. [CrossRef]
36. Henchiri, M.; Igbawua, T.; Javed, T.; Bai, Y.; Zhang, S.; Essifi, B.; Ujoh, F.; Zhang, J. Meteorological Drought Analysis and Return Periods over North and West Africa and Linkage with El Niño–Southern Oscillation (Enso). *Remote Sens.* **2021**, *13*, 4730. [CrossRef]
37. Sun, Y.; Solomon, S.; Dai, A.; Portmann, R.W. How Often Does It Rain? *J. Clim.* **2006**, *19*, 916–934. [CrossRef]
38. Dracup, J.A.; Lee, K.S.; Paulson, E.G. On Definitions of Droughts. *WATER Resour. Res.* **1980**, *16*, 297–302. [CrossRef]
39. Mishra, A.K.; Singh, V.P. Drought Modeling—A Review. *J. Hydrol.* **2011**, *403*, 157–175. [CrossRef]
40. AghaKouchak, A. A Multivariate Approach for Persistence-Based Drought Prediction: Application to the 2010—2011 East Africa Drought. *J. Hydrol.* **2015**, *526*, 127–135. [CrossRef]
41. Soydan Oksal, N.G. Comparative Analysis of the Influence of Temperature and Precipitation on Drought Assessment in the Marmara Region of Turkey: An Examination of SPI and SPEI Indices. *J. Water Clim. Chang.* **2023**, *14*, 3096–3111. [CrossRef]
42. McKee, T.B.; Doesken, N.J.; Kleist, J. The Relationship of Drought Frequency and Duration to Time Scales. In Proceedings of the Eighth Conference on Applied Climatology, Anaheim, CA, USA, 17–22 January 1993; pp. 179–184.
43. Vicente-Serrano, S.M.; Beguería, S.; López-Moreno, J.I. A Multiscalar Drought Index Sensitive to Global Warming: The Standardized Precipitation Evapotranspiration Index. *J. Clim.* **2010**, *23*, 1696–1718. [CrossRef]
44. Spinoni, J.; Naumann, G.; Vogt, J.V.; Barbosa, P. The Biggest Drought Events in Europe from 1950 to 2012. *J. Hydrol. Reg. Stud.* **2015**, *3*, 509–524. [CrossRef]
45. Dukat, P.; Bednorz, E.; Ziemblińska, K.; Urbaniak, M. Trends in Drought Occurrence and Severity at Mid-Latitude European Stations (1951–2015) Estimated Using Standardized Precipitation (SPI) and Precipitation and Evapotranspiration (SPEI) Indices. *Meteorol. Atmos. Phys.* **2022**, *134*, 1–21. [CrossRef]
46. Gurrapu, S.; Chipanshi, A.C.; Sauchyn, D.; Howard, A. Comparison of the SPI and SPEI on Predicting Drought Conditions and Streamflow in the Canadian Prairies. In Proceedings of the 28th Conference on Hydrology—94th American Meteorological Society Annual Meeting, Atlanta, GA, USA, 2–6 February 2014.
47. Tefera, A.S.; Ayoade, J.O.; Bello, N.J. Comparative Analyses of SPI and SPEI as Drought Assessment Tools in Tigray Region, Northern Ethiopia. *SN Appl. Sci.* **2019**, *1*, 265. [CrossRef]
48. Agoussine, M.; El, M.; Saidi, M.; Igmoullan, B.; Ayyad, U.C.; Géosciences, L. De Reconnaissance Des Ressources En Eau Du Bassin d ' Ouarzazate. *Bull. l'Institut Sci. Rabat Sect. Sci. Terre* **2004**, *26*, 81–92.
49. Schulz, O.; Finckh, M.; Goldbach, H. Hydro-Meteorological Measurements in the Drâa Catchment. In *Impacts of Global Change on the Hydrological Cycle in West and Northwest Africa*; Springer: Berlin/Heidelberg, Germany, 2010; pp. 122–131. ISBN 9783642129568.
50. Schulz, O.; Busche, H.; Benbouziane, A. Decadal Precipitation Variances and Reservoir Inflow in the Semi-Arid Upper Drâa Basin (South-Eastern Morocco). In *Environmental Science and Engineering*; Springer: Berlin/Heidelberg, Germany, 2008; pp. 166–178.
51. Ait Ahmad, M. *The Upstream Part of the Oued Draa Watershed: Contribution to the Hydroclimatic and Hydrogeomorphological Study of a Semi-Arid Atlasic*; Faculty of Arts and Humanities, University Ibn Zohr: Agadir, Morocco, 2019.
52. Klose, A. Soil Characteristics and Soil Erosion by Water in a Semi-Arid Catchment (Wadi Drâa, South Morocco) under the Pressure of Global Change. Ph.D. Thesis, Faculty of Mathematics and Sciences, University of Bonn, Bonn, Germany, 2009. Available online: http://hss.ulb.uni-bonn.de/2009/1959/1959.htm (accessed on 24 September 2023).
53. Cappy, S. *Hydrogeological Characterization of the Upper Drâa Catchment: Morocco*; Universitäts-und Landesbibliothek Bonn: Bonn, Germany, 2006.
54. Hussain, F.; Nabi, G.; Waseem Boota, M. Rainfall Trend Analysis By Using the Mann-Kendall Test & Sen'S Slope Estimates: A Case Study of District Chakwal Rain Gauge, Barani Area, Northern Punjab Province, Pakistan. *Sci. Int.* **2015**, *27*, 3159–3165.
55. Sen, P.K. Estimates of the Regression Coefficient Based on Kendall's Tau. *J. Am. Stat. Assoc.* **1968**, *63*, 1379–1389. [CrossRef]

56. Said, A.; Ahmed, A. Drought Variability in Agadir's Region (Southern Morocco)—Recent and Future Trends. *Ecol. Eng. Environ. Technol.* **2023**, *24*, 241–250. [CrossRef]
57. Acharki, S.; Singh, S.K.; do Couto, E.V.; Arjdal, Y.; Elbeltagi, A. Spatio-Temporal Distribution and Prediction of Agricultural and Meteorological Drought in a Mediterranean Coastal Watershed via GIS and Machine Learning. *Phys. Chem. Earth* **2023**, *131*, 103425. [CrossRef]
58. Driouech, F.; ElRhaz, K.; Moufouma-Okia, W.; Arjdal, K.; Balhane, S. Assessing Future Changes of Climate Extreme Events in the CORDEX-MENA Region Using Regional Climate Model ALADIN-Climate. *Earth Syst. Environ.* **2020**, *4*, 477–492. [CrossRef]
59. An, S.; Park, G.; Jung, H.; Jang, D. Assessment of Future Drought Index Using SSP Scenario in Rep. of Korea. *Sustainability* **2022**, *14*, 4252. [CrossRef]
60. Ndayiragije, J.M.; Li, F. Monitoring and Analysis of Drought Characteristics Based on Climate Change in Burundi Using Standardized Precipitation Evapotranspiration Index. *Water* **2022**, *14*, 2511. [CrossRef]
61. Montes-Vega, M.J.; Guardiola-Albert, C.; Rodríguez-Rodríguez, M. Calculation of the SPI, SPEI, and GRDI Indices for Historical Climatic Data from Doñana National Park: Forecasting Climatic Series (2030–2059) Using Two Climatic Scenarios RCP 4.5 and RCP 8.5 by IPCC. *Water* **2023**, *15*, 2369. [CrossRef]
62. Yevjevich, V. An Objective Approach to Definitions and Investigations of Continental Hydrologic Droughts. *J. Hydrol.* **1969**, *7*, 353. [CrossRef]
63. Fritzsche, P. *Development of a Satellite-Based Dynamic Regional Vegetation Model for the Drâa Catchment*; Rheinische Friedrich-Wilhelms-Universität Bonn: Bonn, Germany, 2010.
64. Pepin, N.C.; Arnone, E.; Gobiet, A.; Haslinger, K.; Kotlarski, S.; Notarnicola, C.; Palazzi, E.; Seibert, P.; Serafin, S.; Schöner, W.; et al. Climate Changes and Their Elevational Patterns in the Mountains of the World. *Rev. Geophys.* **2022**, *60*, e2020RG000730. [CrossRef]
65. Bouizrou, I.; Aqnouy, M.; Bouadila, A. Spatio-Temporal Analysis of Trends and Variability in Precipitation across Morocco: Comparative Analysis of Recent and Old Non-Parametric Methods. *J. Afr. Earth Sci.* **2022**, *196*, 104691. [CrossRef]
66. Alemu, M.M.; Bawoke, G.T. Analysis of Spatial Variability and Temporal Trends of Rainfall in Amhara Region, Ethiopia. *J. Water Clim. Chang.* **2020**, *11*, 1505–1520. [CrossRef]
67. Asfaw, A.; Simane, B.; Hassen, A.; Bantider, A. Variability and Time Series Trend Analysis of Rainfall and Temperature in Northcentral Ethiopia: A Case Study in Woleka Sub-Basin. *Weather Clim. Extrem.* **2018**, *19*, 29–41. [CrossRef]
68. Eddoughri, F.; Lkammarte, F.Z.; El Jarroudi, M.; Lahlali, R.; Karmaoui, A.; Yacoubi Khebiza, M.; Messouli, M. Analysis of the Vulnerability of Agriculture to Climate and Anthropogenic Impacts in the Beni Mellal-Khénifra Region, Morocco. *Sustainability* **2022**, *14*, 13166. [CrossRef]
69. Brahim, Y.A.; Saidi, M.E.M.; Kouraiss, K.; Sifeddine, A.; Bouchaou, L. Analysis of Observed Climate Trends and High Resolution Scenarios for the 21st Century in Morocco. *J. Mater. Environ. Sci.* **2017**, *8*, 1375–1384.
70. Rotnicka, J.; Malik, I.; Maciej, D. Simultaneous Growth Releases and Reductions among Populus Alba as an Indicator for Floods in Dry Mountains (Morocco). *Ecol. Indic. J.* **2021**, *129*, 107874. [CrossRef]
71. Rojan, E.; Dłużewski, M.; Krzemień, K. Sediment Budget of High Mountain Stream Channels in an Arid Zone (High Atlas Mountains, Morocco). *Catena* **2020**, *190*, 104530. [CrossRef]
72. Graf, K. *Drinking Water Supply in the Middle Drâa Valley, South Morocco. Options for Action in the Context of Water Scarcity and Institutional Constraints*; Universität zu Köln: Köln, Germany, 2010.
73. Morante-Carballo, F.; Montalván-Burbano, N.; Quiñonez-Barzola, X.; Jaya-Montalvo, M.; Carrión-Mero, P. What Do We Know about Water Scarcity in Semi-Arid Zones? A Global Analysis and Research Trends. *Water* **2022**, *14*, 2685. [CrossRef]
74. Berger, E.; Bossenbroek, L.; Beermann, A.J.; Schäfer, R.B.; Znari, M.; Riethmüller, S.; Sidhu, N.; Kaczmarek, N.; Benaissa, H.; Ghamizi, M.; et al. Social-Ecological Interactions in the Draa River Basin, Southern Morocco: Towards Nature Conservation and Human Well-Being Using the IPBES Framework. *Sci. Total Environ.* **2021**, *769*, 144492. [CrossRef] [PubMed]
75. Xoplaki, E. *Climate Variability over the Mediterranean*; Inauguraldissertation der Philosophisch-naturwissenschaftlichen Fakultät der Universität Bern: Bern, Switzerland, 2002.
76. Lamb, P.J.; Peppler, R.A. North Atlantic Oscillation: Concept and an Application. *Bull. Am. Meteorol. Soc.* **1987**, *68*, 1218–1225. [CrossRef]
77. Trigo, R.M.; Pozo-Vázquez, D.; Osborn, T.J.; Castro-Díez, Y.; Gámiz-Fortis, S.; Esteban-Parra, M.J. North Atlantic Oscillation Influence on Precipitation, River Flow and Water Resources in the Iberian Peninsula. *Int. J. Climatol.* **2004**, *24*, 925–944. [CrossRef]